Material forces: An insight into configurational energy

Francesco Parisio[a], Dmitri Naumov[a], Olaf Kolditz[a,b], Thomas Nagel[a,c,*]

[a] *Department of Environmental Informatics, Helmholtz Centre for Environmental Research – UFZ, Leipzig, Germany*
[b] *Applied Environmental Systems Analysis, Technische Universität Dresden, Dresden, Germany*
[c] *Department of Mechanical and Manufacturing Engineering, School of Engineering, Trinity College Dublin, College Green, Dublin, Ireland*

Abstract

The concept of material or configurational forces, albeit not new, is one of those innovations in theoretical mechanics that has struggled to reach the success of wide-spread acceptance, or even familiarity. Perhaps, one reason for this is to be found in the few available introductory examples or in the non-trivial physical-mathematical approach often taken to establish this concept, although by no means more complex than other treatments in non-linear continuum mechanics. With this work we aim at contributing to the dissemination of configurational mechanics concepts by guiding the reader through an introductory analytical example step by step and comparing it to numerically obtained results. The numerical model is solved with OpenGeoSys (OGS-6), an open-source, C++-based, object-oriented finite element platform for the thermo-hydro-mechanical analysis of coupled processes in fractured porous media. In the spirit of the open-source philosophy, and to enable the readers to reproduce the example themselves, both the source code and the input files are available online. The example highlights—in a simple and intuitive manner—several insightful aspects related to configurational mechanics.

Keywords: Material mechanics, configurational forces, bar with defects, interface effects, OpenGeoSys

1. Configurational forces

The theory of configurational or material forces[1] has provided valuable analysis concepts in many branches of material science and engineering, especially the treatment of defects and inhomogeneities. In his 2005 paper on self-driven dislocations, Epstein summarizes this as follows: [2] "That the Eshelby stress is, at least in part, at the very root of the motion of material defects and other inhomogeneities is a thermodynamic truth that few people doubt, although different people arrive at this conclusion in somewhat different ways". Maugin [1] states that the "unifying notion of material force [..] gathers under one vision all types of driving 'forces' on defects and smooth or abrupt inhomogeneities in fracture, defect mechanics, elastodynamics (localized solutions) and allied theories such as in electroelasticity, magnetoelasticity, and the propagation of phase transition fronts".

Based on these loose definitions it is not surprising that configurational forces or the Eshelby stress tensor (also called energy–momentum tensor) have been used to describe inelastic effects such as elasto-plasticity [3], damage in engineering materials [4, 5], remodelling of biological tissues [6, 7], shear-band formation [8], the contribution of plastic or viscous material effects to fracture [9], and many others. Other examples of usage include h- or r-adaptivity in finite element settings based on configurational forces associated with discretization errors [3, 10]. Especially in finite-strain settings, the occurrence of the Eshelby stress tensor is strongly linked to the multiplicative decomposition of the deformation gradient into inelastic and elastic parts [3, 6]. This example illustrates that considering finite strains in the derivation

*Corresponding author at Department of Environmental Informatics, Helmholtz Centre for Environmental Research – UFZ, Leipzig, Germany. thomas.nagel@ufz.de

[1] Known under many synonyms in the context of related concepts, such as suction force in a cracked body, force on an elastic singularity, force on an elastic defect, force on a dislocation, inhomogeneity force, crack extension force, driving force on a soliton, force on an interface, Γ-invariant integrals, J-integral of fracture, etc. [1].

of configurational effects, even if the subsequently employed theory is limited to linear kinematics, is generally advised since premature linearization can obscure physical effects routed in higher-order space-time derivatives; cf. also Ref. [1].

The existence of configurational forces has recently been demonstrated by a series of clever experiments that highlight Eshelby-like forces in elastic structures [11], demonstrate the possibility of torsional locomotion [12] and show interesting applications related to serpentine locomotion [13] and mixed equilibrium-deformation scale [14].

Despite its interpretative value for a wide range of physical and engineering analyses, the idea of material forces remains isolated and access to the topic can be hampered by the advanced and highly mathematical nature of many key references. The aim of this contribution is to provide an introductory example by analyzing a simple, yet illustrative analytical and numerical application of material forces to an inhomogeneous elastic material loaded in a one-dimensional setting. We have implemented the assembly of material force vectors into the open-source FEM code OpenGeoSys[2] [15, 16], which we will use to analyze the distribution of material forces the heterogeneous continuum and compare the results to those obtained from the analytical solution.

The notion of configurational forces can be arrived at from different angles, such as a pull-back of the physical momentum balance to the reference configuration [1], invariance considerations and conservation principles [17], or the introduction of an additional balance law related to phenomena on the micro-scale [18].

An intuitive access can be gained by considering a possible motion of an inhomogeneity in an elastic material. Such a motion relative to the reference configuration is associated with a change in the elastic energy of the system. Configurational forces are the work-conjugate drivers of this motion. Extending this thought experiment by considering that plastic deformation is strongly linked to the motion of dislocations on the micro-scale which can macroscopically be thought of as continuously distributed defects, "it becomes obvious that the Eshelby stress is work conjugate to the rate of the plastic deformation by the dissipation inequality" [3].

In a dissipative and quasi-static context, we choose here the illustrative approach of expanding the gradient of the free Helmholtz energy density $\psi(\mathbf{F}, \boldsymbol{\kappa}, \kappa; \mathbf{X})$, where $\mathbf{F}$ is the deformation gradient, $\boldsymbol{\kappa}$ and κ represent tensorial and scalar internal variables, and the dependence on the position vector $\mathbf{X}$ signifies as usual the explicit incorporation of inhomogeneities:

$$\begin{aligned}\operatorname{Grad}\psi = \frac{\partial\psi}{\partial\mathbf{F}} : \operatorname{Grad}\mathbf{F} + \frac{\partial\psi}{\partial\boldsymbol{\kappa}} : \operatorname{Grad}\boldsymbol{\kappa} + \\ + \frac{\partial\psi}{\partial\kappa}\operatorname{Grad}\kappa + \left.\frac{\partial\psi}{\partial\mathbf{X}}\right|_{\text{expl.}}.\end{aligned} \tag{1}$$

In terms of notation, operators with capital letters such as Grad $(\bullet)$ and Div $(\bullet)$ represent differential operators with respect to the reference configuration (material coordinates $\mathbf{X}$) and lower-case operators such as grad $(\bullet)$ and div $(\bullet)$ operate on the current configuration (spatial coordinates $\mathbf{x}$).

From the isothermal Clausius-Planck inequality in a standard setting, one can derive the driving forces of the internal variables (sometime referred to as associated thermodynamic forces) $\mathbf{Y}_{\boldsymbol{\kappa}}$, Y_κ as well as find the standard definition of the first Piola-Kirchhoff stress tensor $\mathbf{P}$

$$0 \leq \mathbf{P} : \dot{\mathbf{F}} - \dot{\psi}, \tag{2}$$

or, expanded,

$$0 \leq \left(\mathbf{P} - \frac{\partial\psi}{\partial\mathbf{F}}\right) : \dot{\mathbf{F}} - \frac{\partial\psi}{\partial\boldsymbol{\kappa}} : \dot{\boldsymbol{\kappa}} - \frac{\partial\psi}{\partial\kappa}\dot{\kappa}, \tag{3}$$

where the residual dissipation inequality reads

$$\mathcal{D} = \mathbf{Y}_{\boldsymbol{\kappa}} : \dot{\boldsymbol{\kappa}} + Y_\kappa\dot{\kappa} \geq 0, \tag{4}$$

with

$$\mathbf{Y}_{\boldsymbol{\kappa}} = -\frac{\partial\psi}{\partial\boldsymbol{\kappa}}\,;\; Y_\kappa = -\frac{\partial\psi}{\partial\kappa}\,;\; \mathbf{P} = \frac{\partial\psi}{\partial\mathbf{F}}. \tag{5}$$

With these definitions, Eq. (1) can be rearranged by virtue of the chain rule and Young's theorem to

$$\begin{aligned}\mathbf{0} = \operatorname{Div}(\psi\mathbf{I} - \mathbf{F}^{\mathrm{T}}\mathbf{P}) + \mathbf{F}^{\mathrm{T}}\operatorname{Div}\mathbf{P} + \\ + \mathbf{Y}_{\boldsymbol{\kappa}} : \operatorname{Grad}\boldsymbol{\kappa} + Y_\kappa\operatorname{Grad}\kappa - \left.\frac{\partial\psi}{\partial\mathbf{X}}\right|_{\text{expl.}}.\end{aligned} \tag{6}$$

Employing the physical momentum balance in the form $\operatorname{Div}\mathbf{P} + \rho_0\mathbf{b} = \mathbf{0}$ and defining the energy-momentum or Eshelby tensor as $\boldsymbol{\Sigma} = \psi\mathbf{I} - \mathbf{F}^{\mathrm{T}}\mathbf{P}$ yields the configurational force balance

$$\mathbf{0} = \operatorname{Div}\boldsymbol{\Sigma} + \mathbf{g}, \tag{7}$$

[2] www.opengeosys.org

with

$$\mathbf{g} = \mathbf{g}_{\text{diss}} + \mathbf{g}_{\text{vol}} + \mathbf{g}_{\text{inh}}, \tag{8}$$

and

$$\begin{aligned} \mathbf{g}_{\text{diss}} &= \mathbf{Y}_{\boldsymbol{\kappa}} : \operatorname{Grad} \boldsymbol{\kappa} + Y_{\kappa} \operatorname{Grad} \kappa \\ \mathbf{g}_{\text{vol}} &= -\rho_0 \mathbf{F}^{\mathrm{T}} \mathbf{b} \\ \mathbf{g}_{\text{inh}} &= -\left. \frac{\partial \psi}{\partial \mathbf{X}} \right|_{\text{expl.}} \end{aligned} \tag{9}$$

These contributions make apparent that configurational forces arise as a consequence of inhomogeneous dissipative effects, of body-forces $\mathbf{b}$ in conjunction with heterogeneous displacement fields, and in the presence of distinct inhomogeneities.

To arrive at a small-strain setting, spatial differential operators with respect to the reference coordinates $\mathbf{X}$ are replaced by the operators div and grad with respect to the coordinates $\mathbf{x}$ as well as re-defining the Eshelby stress and the volumetric contribution as

$$\boldsymbol{\Sigma} = \psi \mathbf{I} - \operatorname{grad}^{\mathrm{T}} \mathbf{u}\, \boldsymbol{\sigma} \tag{10}$$

and

$$\mathbf{g}_{\text{vol}} = -\varrho \operatorname{grad}^{\mathrm{T}} \mathbf{u}\, \mathbf{b} \tag{11}$$

in terms of the Cauchy stress tensor $\boldsymbol{\sigma}$ and the displacement gradient. For the finite element implementation (compare reference [19]), a test function $\mathbf{v} \in \mathbf{V}_0$ is chosen such that

$$\mathbf{V}_0 = \left\{ \mathbf{v} \in H^1(\Omega) : \mathbf{v} = \mathbf{0} \;\forall\; \mathbf{x} \in \partial\Omega \right\}. \tag{12}$$

in order to arrive at the weak form of the configurational force balance

$$\int_{\Omega} \left(\boldsymbol{\Sigma} : \operatorname{grad} \mathbf{v} - \mathbf{g} \cdot \mathbf{v} \right) \mathrm{d}\Omega = 0. \tag{13}$$

Now, a nodal material force vector can be assembled from the discretized Eshelby-stress integral

$$\underline{F}_{\text{conf}} = \int_{\Omega} \underline{\underline{N}}^{\mathrm{T}} \underline{g}\, \mathrm{d}\Omega = \int_{\Omega} \underline{\underline{G}}^{\mathrm{T}} \underline{\Sigma}\, \mathrm{d}\Omega. \tag{14}$$

In the above, $\underline{\underline{N}}$ and $\underline{\underline{G}}$ are suitably defined shape-function matrices and gradient matrices, respectively, while $\underline{\Sigma}$ is a vectorial representation of the Eshelby stress tensor coordinates[3]. Regarding the implementation into OpenGeoSys, these definitions follow those outlined in Nagel et al. [16] for the displacement gradient etc.

[3] Note that due to $\boldsymbol{\Sigma} \neq \boldsymbol{\Sigma}^{\mathrm{T}}$ this is a nine-dimensional vector in a three-dimensional setting.

2. Heterogeneous bar under tensile loading

2.1. Analytical solution

The example is designed to illustrate some of the basic concepts of material forces. First, consider a bar made of a linearly elastic material loaded in uniaxial tension/compression (no lateral stresses) under constant stress σ_0 in the small strain range. The Young's modulus of the material is linearly distributed along the bar around its average mid-point value E_0

$$E(x) = E_0 \left[1 + \alpha \left(\frac{x}{l} - \frac{1}{2} \right) \right]. \tag{15}$$

One possible interpretation relates stiffness linearly to $\tilde{\phi}_{\text{v}}(x)$ as

$$E(x) = \left[1 - \tilde{\phi}_{\text{v}}(x) \right] E_0, \tag{16}$$

where $\tilde{\phi}_{\text{v}}(x)$ could be a volumetric measure of void or defect density

$$\tilde{\phi}_{\text{v}}(x) = \alpha \left(\frac{1}{2} - \frac{x}{l} \right). \tag{17}$$

In that sense, $\tilde{\phi}_{\text{v}}$ is not an absolute measure but expresses the void density relative to a base-line value corresponding to E_0 in the centre of the bar. Due to the linear distribution anchored in the centre of the bar, the total void density is a conserved quantity, i.e.

$$\tilde{\Phi}_{\text{v}} = \int_0^l \tilde{\phi}_{\text{v}}(x)\, \mathrm{d}x = 0 \tag{18}$$

holds for the total deviation. The physically meaningful interval for the slope is $\alpha \in (-2, 2)$, so that $\tilde{\phi}_{\text{v}}(x) \in (0, 1)$.

We recall that the dissipative contribution g_{diss} is null for elastic materials and that we do not consider volumetric forces, so that $g_{\text{vol}} = 0$. Hence,

$$g_{\text{inh}} = -\operatorname{div} \Sigma \tag{19}$$

holds. The gradient of the displacement field along the bar reads

$$\operatorname{grad} u = \epsilon = \frac{\sigma_0}{E_0} \left[1 + \alpha \left(\frac{x}{l} - \frac{1}{2} \right) \right]^{-1}, \tag{20}$$

and the free energy per unit volume

$$\psi = \frac{1}{2} \sigma \epsilon = \frac{\sigma_0^2}{2 E_0} \left[1 + \alpha \left(\frac{x}{l} - \frac{1}{2} \right) \right]^{-1}. \tag{21}$$

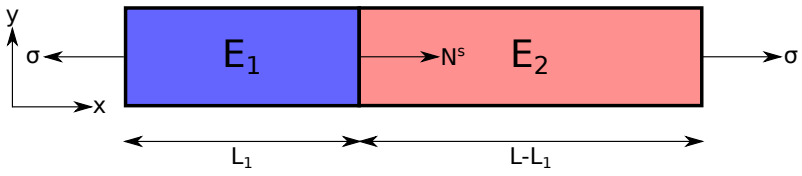

Figure 1: Schematic representation of a bi-material bar (different stiffness in this case) under tensile load.

Hence, $\Sigma = -\psi$ and we can, in conjunction with Eq. (19), compute the material forces per unit volume as

$$g_{\text{inh}} = -\operatorname{div}\Sigma = \\ = -\frac{\alpha\sigma_0^2}{2E_0 l}\left[1+\alpha\left(\frac{x}{l}-\frac{1}{2}\right)\right]^{-2}. \tag{22}$$

2.2. Integration of material forces

The vectorial field of the material forces $\underline{G}_{\text{inh}}$ is computed as a post-processed variable and is defined at the nodes of the finite element discretization as a result of the integration over the adjacent elements' volumes as expressed in Eq. (14). The computation is analogous to the calculation of nodal reactions $\underline{R}_i$ based on Cauchy's stresses. As in the standard FEM procedure, equilibrium of momentum implies vanishing nodal reactions $\underline{R}_i$ except at traction boundaries. The physical meaning of the un-balanced component of the material force vector field at the internal nodes of the domain is illustrated at the end of this section. Due to an element-wise assignment of the Young's modulus, the comparison with the analytical solution has to consider the discretization of the problem in the sense of a sequel of material-domain interfaces. For illustration, let us first consider an interface between two solids with different Young's moduli in a uniaxial stress field as shown in Fig. 1. The plane separating the two regions Ω_1 and Ω_2 of the domain Ω (bounded by $\partial\Omega$) is an oriented surface with a unit normal $\mathbf{N}^{\text{S}}$ pointing into material 2. Allowing a jump of Eshelby's stress $\boldsymbol{\Sigma}$ at the interface we have

$$\int_{\partial\Omega}\boldsymbol{\Sigma}\cdot\mathbf{N}\mathrm{d}\Gamma = \\ = \int_{\Omega_1\cup\Omega_2}\operatorname{Div}\boldsymbol{\Sigma}\mathrm{d}\Omega + \int_{\text{S}}[\![\boldsymbol{\Sigma}]\!]\cdot\mathbf{N}^{\text{S}}\mathrm{d}\Gamma, \tag{23}$$

where

$$[\![\bullet]\!] = (\bullet)|_2 - (\bullet)|_1, \tag{24}$$

defines a jump in quantity $\bullet$ over the boundary between the two material domains. The total material force $\mathbf{G}$ at the interface can be computed as

$$\mathbf{G} = -\int_{\text{S}}[\![\boldsymbol{\Sigma}]\!]\cdot\mathbf{N}^{\text{S}}\mathrm{d}\Gamma \tag{25}$$

whereas the individual domains remain divergence-free. As we have defined the problem to be uniaxial, the only non-zero component of Eshelby's stress Σ at material domain 1 and 2 is

$$\Sigma_1 = -\frac{\sigma^2}{2E_1} \quad \text{and} \quad \Sigma_2 = -\frac{\sigma^2}{2E_2}, \tag{26}$$

with E_1 and E_2 being the Young's modulus of domain 1 and 2 respectively, so that the material force at the interface is given as

$$G = -\int_{\text{S}}[\![\Sigma]\!]\mathrm{d}\Gamma = -[\![\Sigma]\!]A = \\ = -\frac{\sigma^2\left(E_2-E_1\right)}{2E_1E_2}A, \tag{27}$$

where A is the cross section area of the bar. The same result can be arrived at by energetic arguments in which the total elastic potential equal to the mechanical work is defined as

$$\Psi = \int_{\Omega}\psi\,\mathrm{d}\Omega = W = \frac{1}{2}Fu = \\ = \frac{1}{2}\sigma A\left[\varepsilon_1 L_1 - \varepsilon_2\left(L-L_1\right)\right], \tag{28}$$

from which the material force is obtained via the variation of energy with respect to the position of the interface between domain 1 and domain 2

$$G = -\frac{\partial W}{\partial L_1} = -\frac{1}{2}F\left(\varepsilon_1-\varepsilon_2\right) = \\ = -\frac{\sigma^2\left(E_2-E_1\right)}{2E_1E_2}A. \tag{29}$$

From the previous results it can be observed how the material force acting on the interface depends on the stiffness difference between the two materials $E_2 - E_1$. More specifically, the sign and therefore

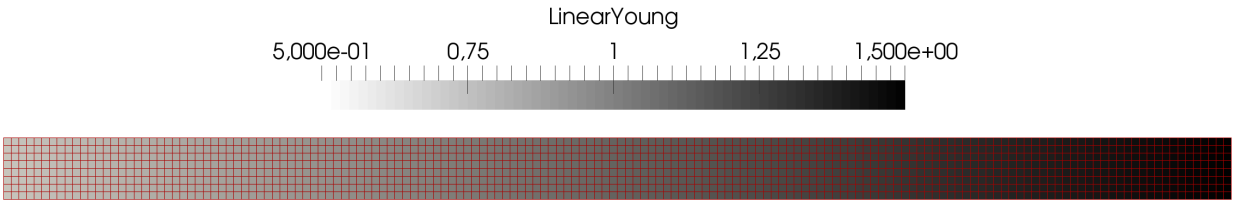

Figure 2: Mesh of the finite element model and distribution of Young's modulus in the bar.

the direction of the forces will be determined by this difference. This example can be directly extended to account for a piece-wise constant approximation of a linear distribution in which many interfaces exist inside the solid, each of which is the boundary between two adjacent elements in an FEM discretization.

2.3. Numerical model

The problem that is solved numerically consists of a linear elastic bar of unit length and a width of 0.05 m that has a linear distribution of Young's modulus as in Eq. (15) with $\alpha = 1$, $E_0 = 1\,\mathrm{GPa}$ and $l = 1\,\mathrm{m}$. The mesh is regular and comprised of bi-linear quadrilateral elements of fixed edge length of 0.00625 m. The mesh and Young's modulus distribution are illustrated in Fig. 2. The left-hand side is a fixed end with constrained horizontal displacement, the right-hand side constitutes a traction boundary with an applied tensile stress $\sigma = 0.01\,\mathrm{GPa}$. Vertical displacements are fixed at both the bottom right and left nodes to avoid rigid body movements. The problem is solved in two-dimensional plane-strain conditions and the Poisson's ratio is set to zero to avoid lateral deformations and stresses. The version of OpenGeoSys employed is available at[4]
https://github.com/fparisio/ogs/tree/SVOSDN_MF_BB
and the input files (bar.vtu, bar.gml and bar.prj) can be found in the source code in the directory `/src/Tests/Data/Mechanics/Linear/`.

To compare analytical and numerical results, let us now consider a bar with a linear distribution of stiffness as represented in the numerical example. Because the Young's modulus in the present finite element model is defined as an element property, the distribution is a stepwise function in which the step size depends on the spatial discretization of the problem. Fig. 3(a) shows the comparison between analytical distribution of Young's modulus and the FEM distribution in OpenGeoSys.

Based on the above considerations, the analytical solution of the material forces at a cross-section x can be obtained in two different ways: firstly, by using the analytical solution of the bimaterial interface from Eq. (27) with a discretization that corresponds to the FEM mesh illustrated in Fig. 2, i.e., $\Delta x = 0.00625\,\mathrm{m}$. At the interface between two consecutive elements, we can write the total material force G_i using Eq. (27) as

$$G_i = -\frac{\sigma^2 \left[E|_{x_i+\frac{\Delta x}{2}} - E|_{x_i-\frac{\Delta x}{2}}\right]}{2E|_{x_i+\frac{\Delta x}{2}} E|_{x_i-\frac{\Delta x}{2}}} A, \tag{30}$$

where x_i is the position of the interface between the two domains.

Secondly, one can integrate the specific body force from Eq. (22) over the volume surrounding each discrete interface to obtain

$$G_i = -\frac{\alpha\sigma_0^2}{2E_0 l}\left[1 + \alpha\left(\frac{x_i}{l} - \frac{1}{2}\right)\right]^{-2} A\Delta x. \tag{31}$$

The integral of Eq. (31) is computed assuming a sufficiently fine discretization that g_{inh} can be considered to be linear in the proximity of the interface.

3. Results

Fig. 3(b) illustrates the comparison of the two analytical methods, leading to coinciding curves and thus showing that the body force-derived solution corresponds to the interface-based one. Fig. 3(c) shows the comparison between the nodal material forces obtained from the analytical solution and the numerical computation with OpenGeoSys[5] as a function of the coordinate x. Except for boundary effects, which are not considered due to $\delta\mathbf{X}|_{\partial\Omega} = 0$, the comparison is

[4] As part of the usual development process, the feature will soon become part of the official main version of the software.

[5] Note, that to obtain the total material force acting on a given cross section the axial components of all material force vectors in this cross section need to be summed up.

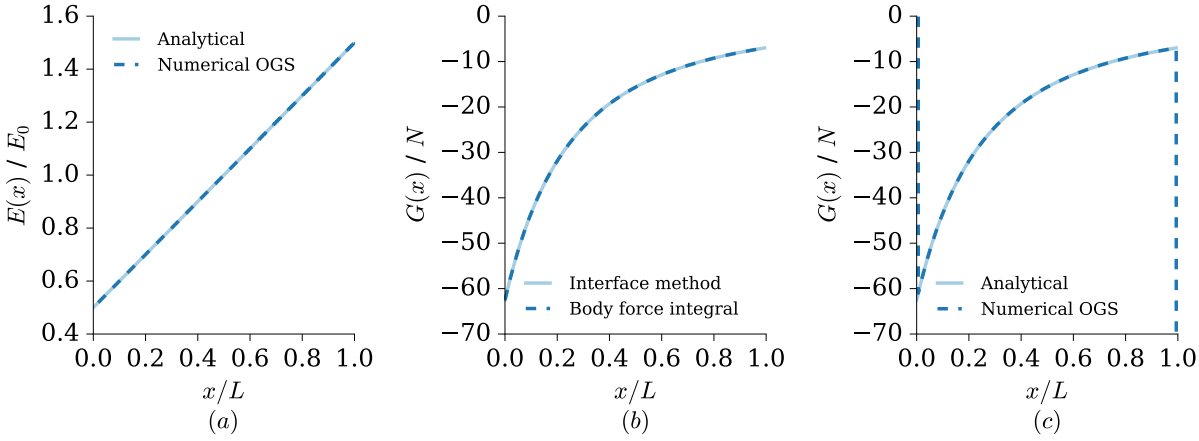

Figure 3: Example for material forces acting in an inhomogeneous bar under tension: the continuous analytical distribution of the Young's modulus and the discrete distribution serving as input for OpenGeoSys (a); the discretized material force distribution obtained as total forces G_i from the material interface equilibrium (Eq. (30)) or as integral of material force density (Eq. (31)) (b); comparison between the analytical solution and the result from the analysis with OpenGeoSys (c).

consistent and verifies the OpenGeoSys implementation.

In the void interpretation that was previously introduced, the material is denser at the right-hand side which accordingly elicits a stiffer response. In the context of this interpretation, and based on the obtained results, the material or configurational force field acts as a driving force for the migration of voids (or, alternatively and reversely, stiffness, i.e., material points) from left to right in an effort to re-establish a configuration with smaller overall elastic potential energy. In other words, the driver for this migration are configurational changes that aim at minimizing the energy in the system

$$\Psi = \int_0^l \psi(x) A \mathrm{d}x = \frac{\sigma_0^2 A l}{2 E_0 \alpha} \ln \frac{2+\alpha}{2-\alpha}. \tag{32}$$

To find the configuration with minimal elastic energy we use

$$\frac{\mathrm{d}\Psi}{\mathrm{d}\alpha} = 0 = -\frac{(\alpha^2-4)\ln\frac{2+\alpha}{2-\alpha} + 4\alpha}{\alpha^2(\alpha^2-4)}, \tag{33}$$

so that in the physically relevant interval we find

$$\bar{\alpha} = \underset{\alpha\in(-2,2)}{\arg\min}\, \Psi = 0. \tag{34}$$

We see that a configurational rearrangement towards homogeneity is energetically beneficial. Additionally, we can see from Eq. (34) that the material forces tend to restore a homogeneous configuration in the present problem which by design conserves the mean stiffness/void density. That is, the stiffness distribution simply rotates around its middle-point value (which corresponds to the average throughout the bar) without any translation. If we think about voids or defect density, such voids can only be redistributed inside the beam without expulsion through the boundaries. The boundaries, therefore, can be considered as "adiabatic" with respect to inhomogeneities and material points configuration. The interpretation of a configurational force acting on a single material interface as indicated in Fig. 1 and expressed by Eq. (27) shows that the interface has a tendency to move into the stiffer material, thereby softening the bar and minimizing the energy under constant-stress boundary conditions. We close again by remarking that the configurational forces are not to be confused with physical forces, but are an illustrative way of looking at energetic phenomena.

4. Conclusion

We have shown step by step a simple, yet very insightful application of material forces to a mechanical problem. The comparison between numerical simulations and analytical results also verifies the implementation of material-force assembly in the open-source finite element framework OpenGeoSys. The analytical solution can be derived in different ways, either

in a continuously varying setting or in its approximation by a series of discrete material interfaces. In an inhomogeneous bar under tensile loading, material forces have shown to drive the problem toward a lower energetic configuration, acting to restore homogeneity under the conditions considered here. Because of their implied physical meaning, material forces can be a very powerful tool in the hands of modelers which can help to solve numerous complex problems related to the physics of continua. Our goal was to give the reader a simple application example that turns the complex mathematical formulation of material forces into an intuitive physical problem. We have done so in an effort to illustrate the concept of material forces toward other scientific communities that might be less familiar with this non-classical continuum mechanical topic.

5. Acknowledgments

This research was financed by the Helmholtz Association of German Research Centres within the Research Programme Renewable Energies and the GEMex project. The GEMex project is supported by the European Union's Horizon 2020 programme for Research and Innovation under grant agreement No 727550.

6. References

[1] G. A. Maugin, Material Forces: Concepts and Applications, Applied Mechanics Reviews 48 (5) (1995) 213–245. doi:10.1115/1.3005101.

[2] M. Epstein, Self-driven continuous dislocations and growth, in: Mechanics of material forces, Springer, 2005, pp. 129–139.

[3] D. Gross, S. Kolling, R. Mueller, I. Schmidt, Configurational forces and their application in solid mechanics, European Journal of Mechanics - A/Solids 22 (5) (2003) 669 – 692. doi:http://dx.doi.org/10.1016/S0997-7538(03)00076-7.

[4] T. Liebe, R. Denzer, P. Steinmann, Application of the material force method to isotropic continuum damage, Computational Mechanics 30 (3) (2003) 171–184.

[5] M. Timmel, M. Kaliske, S. Kolling, Modelling of microstructural void evolution with configurational forces, ZAMM-Journal of Applied Mathematics and Mechanics/Zeitschrift für Angewandte Mathematik und Mechanik 89 (8) (2009) 698–708.

[6] K. Garikipati, J. Olberding, H. Narayanan, E. Arruda, K. Grosh, S. Calve, Biological remodelling: Stationary energy, configurational change, internal variables and dissipation, Journal of the Mechanics and Physics of Solids 54 (7) (2006) 1493 – 1515. doi:DOI:10.1016/j.jmps.2005.11.011.

[7] T. Nagel, D. Kelly, Remodelling of collagen fibre transition stretch and angular distribution in soft biological tissues and cell-seeded hydrogels., Biomech Model Mechanobiol 11 (3-4) (2012) 325–339. doi:10.1007/s10237-011-0313-3.
URL http://dx.doi.org/10.1007/s10237-011-0313-3

[8] I. Maatouki, R. Müller, D. Gross, Material forces in elasto-plastic materials, PAMM 8 (1) (2008) 10441–10442.

[9] K. Özenç, M. Kaliske, G. Lin, G. Bhashyam, Evaluation of energy contributions in elasto-plastic fracture: a review of the configurational force approach, Engineering Fracture Mechanics 115 (2014) 137–153.

[10] R. Mueller, D. Gross, G. Maugin, Use of material forces in adaptive finite element methods, Computational Mechanics 33 (6) (2004) 421–434.

[11] D. Bigoni, F. Dal Corso, F. Bosi, D. Misseroni, Eshelby-like forces acting on elastic structures: theoretical and experimental proof, Mechanics of Materials 80 (2015) 368–374.

[12] D. Bigoni, F. Dal Corso, D. Misseroni, F. Bosi, Torsional locomotion 470 (2171) (2014) 20140599.

[13] F. Dal Corso, D. Misseroni, N. Pugno, A. Movchan, N. Movchan, D. Bigoni, Serpentine locomotion through elastic energy release, Journal of The Royal Society Interface 14 (130) (2017) 20170055.

[14] F. Bosi, D. Misseroni, F. Dal Corso, D. Bigoni, An elastica arm scale 470 (2169) (2014) 20140232.

[15] O. Kolditz, S. Bauer, L. Bilke, N. Böttcher, J.-O. Delfs, T. Fischer, U. J. Görke, T. Kalbacher, G. Kosakowski, C. McDermott, et al., OpenGeoSys: an open-source initiative for numerical simulation of thermo-hydro-mechanical/chemical (THM/C) processes in porous media, Environmental Earth Sciences 67 (2) (2012) 589–599.

[16] T. Nagel, U.-J. Görke, K. M. Moerman, O. Kolditz, On advantages of the Kelvin mapping in finite element implementations of deformation processes, Environmental Earth Sciences 75 (11) (2016) 1–11. doi:10.1007/s12665-016-5429-4.

[17] R. Kienzler, G. Herrmann, Mechanics in material space: with applications to defect and fracture mechanics, Springer Science & Business Media, 2012.

[18] M. E. Gurtin, Configurational forces as basic concepts of continuum physics, Vol. 137, Springer Science & Business Media, 2008.

[19] R. Mueller, S. Kolling, D. Gross, On configurational forces in the context of the finite element method, International Journal for Numerical Methods in Engineering 53 (7) (2002) 1557–1574.